remote sensing

MDPI

Article

Exploring the Sensitivity of Solar-Induced Chlorophyll Fluorescence at Different Wavelengths in Response to Drought

Shan Xu [1,2,3], Zhigang Liu [1,2,*], Shuai Han [1,2], Zhuang Chen [1,2], Xue He [1,2], Huarong Zhao [4,5] and Sanxue Ren [4,5]

[1] State Key Laboratory of Remote Sensing Science, Faculty of Geographical Science, Beijing Normal University, Beijing 100875, China
[2] Beijing Engineering Research Centre for Global Land Remote Sensing Products, Faculty of Geographical Science, Beijing Normal University, Beijing 100875, China
[3] Plant Phenomics Research Centre, Academy for Advanced Interdisciplinary Studies, Nanjing Agricultural University, Nanjing 210095, China
[4] Chinese Academy of Meteorological Sciences, Beijing 100081, China
[5] Hebei Gucheng Agricultural Meteorology National Observation and Research Station, Baoding 072656, China
* Correspondence: zhigangliu@bnu.edu.cn; Tel.: +86-136-5105-1881

Abstract: Due to the mechanistic coupling between solar-induced chlorophyll fluorescence (SIF) and photosynthesis, SIF has an advantage over greenness-based vegetation indices in detecting drought. Since photosystem I (PSI) contributes very little to red SIF, red SIF is assumed to be more responsive to environmental stress than far-red SIF. However, in addition to affecting photosynthesis, drought also has an impact on vegetation chlorophyll concentration and thus affects the reabsorption process of red SIF. When these responses are entangled, the sensitivity of SIF in the red and far-red regions in response to drought is not yet clear. In this study, we conducted a water stress experiment on maize in the field and measured the upward and downward leaf SIF spectra by a spectrometer assembled with a leaf clip. Simultaneously, leaf-level active fluorescence was measured with a pulse-amplified modulation (PAM) fluorometer. We found that SIF, after normalization by photosynthetically active radiation (PAR) and dark-adapted minimal fluorescence (F_o), is a better estimation of SIF yield. By comparing the wavelength-dependent link between SIF yield and nonphotochemical quenching (NPQ) across the range of 660 to 800 nm, the results show that red SIF and far-red SIF have different sensitivities in response to drought. SIF yield in the far-red region has a strong and stable correlation with NPQ. Drought not only reduces red SIF due to photosynthetic regulation, but it also increases red SIF by reducing chlorophyll content (weakening the reabsorption effect). The co-existence of these two contradictory effects makes the red SIF of leaf level unable to reliably indicate NPQ. In addition, the red:far-red ratio of downward SIF and the ratio between the downward SIF and upward SIF at the red peak can be good indicators of chlorophyll content. These findings can help to interpret SIF variations in remote sensing techniques and fully exploit SIF information in red and far-red regions when monitoring plant water stress.

Keywords: SIF; drought; physiology; absorption; leaf level

Citation: Xu, S.; Liu, Z.; Han, S.; Chen, Z.; He, X.; Zhao, H.; Ren, S. Exploring the Sensitivity of Solar-Induced Chlorophyll Fluorescence at Different Wavelengths in Response to Drought. *Remote Sens.* **2023**, *15*, 1077. https://doi.org/10.3390/rs15041077

Academic Editors: Jochem Verrelst and Won-Ho Nam

Received: 12 December 2022
Revised: 13 February 2023
Accepted: 13 February 2023
Published: 16 February 2023

1. Introduction

Climate change has generally exacerbated drought processes and become more intense in the world [1,2]. Drought often leads to devastating effects on crop yield through negative impacts on plant growth, physiology, and reproduction [3], which has been one of the major constraints to food security worldwide. Therefore, there is an urgent need for a method of early warning of emerging drought on crops that can provide information on the real-time health status of plants for agricultural planning and mitigation. Present insight into drought effects on plants has been gained by fusing vegetation indices (VIs) from remote sensing with climatological dryness indicators such as the Palmer drought

severity index [4]. This combined approach has been widely used to estimate drought severity across space during large-scale droughts [5]. The main limitation of this approach is that greenness-based VIs usually provide estimates of plant status related to structural or biochemical properties and do not capture shorter timescale changes in physiology that occur during a drought episode. Remote sensing of solar-induced chlorophyll fluorescence (SIF) offers the potential to complement existing methods and provide critical physiological information that meets the need for early warning of drought.

Under the illumination of sunlight, part of the energy absorbed by chlorophyll is re-emitted at a longer wavelength than for excitation from the light reactions of photosynthesis, and the energy is dissipated as chlorophyll fluorescence (ChlF) at 650–850 nm. Together with nonphotochemical quenching (NPQ), ChlF competes with photosynthesis for the use of absorbed energy. Due to this close relationship between ChlF and photosynthesis, pulse-amplitude modulated (PAM) fluorescence has long been used by biophysicists and ecophysiologists to elucidate the function of the photosynthetic apparatus but is restricted to the leaf scale [6]. Recent advances in remote sensing of SIF show promise for mapping the drought status of plants across a continuum of spatial scales from the perspective of photosynthesis [7], which is more sensitive to environmental conditions. Typically, ground-based remote sensing of SIF signals is retrieved by exploiting the Fraunhofer line depths at O_2-A and O_2-B at 760 nm and 687 nm, respectively. Our previous studies have demonstrated that ground-based far-red SIF can respond to water stress and reflect variations in the physiological states of crops at the leaf and canopy levels [8,9]. In addition, by comprising SIF measurements in far-red and normalized difference vegetation index (NDVI) data, studies have found that SIF can provides important physiology information [10,11]. Unmanned aerial vehicles and satellite SIF in the far red also showed strong negative anomalies across space [11–13].

Despite the mounting evidence of the negative anomalies of far-red SIF under drought observed from different platforms, the implicated information in other SIF bands remains to be discovered when plants suffer from stress. The SIF spectrum covers the wavelength range from 650 to 800 nm, which has two peaks centered in the red (~685 nm) and far-red (~740 nm) spectra, with nonequal contributions from photosystem I (PSI) and photosystem II (PSII) [14]. PSI fluorescence predominantly in the near infrared bands and is assumed to be constant and lower than the fluorescence of PSII [15,16]. PSII fluorescence ranges from the red to the near infrared spectrum and is regulated by photosynthesis (photochemical quenching, PQ) and NPQ. Since PSI contributes very little to red SIF (~687 nm), red SIF is thought to be more responsive to environmental stress or photosynthesis status (downregulation of PSII) compared to far-red SIF [17,18].

However, the intensity of the SIF signal emitted from a leaf or a plant canopy at a given wavelength (λ) is also driven by physiological (e.g., photosynthesis) and biochemical (e.g., chlorophyll concentration) or canopy structure (e.g., leaf area index) factors accounting for energy absorption and SIF reabsorption or scattering [19], which can be represented using a simple equation:

$$SIF_\lambda = PAR \times fPAR \times \Phi F_\lambda \times fesc_\lambda \quad (1)$$

where PAR is the photosynthetically active radiation; $fPAR$ is the fraction of absorbed incoming PAR; ΦF_λ is the wavelength-dependent fluorescence quantum yield; and $fesc_\lambda$ is the spectrally dependent escape probability from the photosystem to sensors ($fesc_\lambda$). Therefore, there is a need to disentangle the physiological information (ΦF_λ) from SIF_λ by eliminating physical and biochemical factors ($fPAR$ and $fesc_\lambda$). For the far-red SIF region, the escape probability of SIF photons from the photosystems to the leaf surface is rather stable and can be assumed to be a constant [20,21], and the escape probability of SIF photons from the leaf level to the canopy level can be represented as a product of far-red reflectance, canopy interception, and leaf albedo [22]. The red SIF overlaps the spectral range of chlorophyll absorption and is thereby strongly reabsorbed inside the leaf or canopy, which makes the estimation of $fesc_\lambda$ in the red band very difficult. In particular, leaf chlorophyll a and b content (Cab) tends to decrease when plants suffer from drought [23,24]. This

decrease in Cab has the opposite effect on the total absorbed energy and escape probability of red SIF photos; i.e., decreased chlorophyll limits the ability to absorb light by decreasing *fPAR* but increases the escape probability by decreasing reabsorption. By accounting for changes in the spectral shape due to chlorophyll reabsorption, researchers have suggested that the red and far-red SIF ratio can potentially provide information on the responses of vegetation to environmental stress or chlorophyll content [25–28].

As introduced above, the red band SIF is expected to contain more information from PSII, which should be more sensitive to environmental stress than far-red SIF. However, it remains unclear: (1) whether red SIF is more sensitive to drought-induced physiological variation; (2) whether the red and far-red SIF ratio can be used as a simple indicator of physiological variation or chlorophyll content induced by drought; and (3) whether it is possible to correct the reabsorption effect in the red SIF region. Regarding these issues, in this study, a water stress experiment in maize as a case study was used to analyze the sensitivity of entire leaf-level SIF spectra to drought. Leaf-level SIF was used to eliminate the complex effect of canopy structure on SIF. SIF measurements were performed with a spectroradiometer coupled with the FluoWat leaf clip. This leaf clip is able to measure real leaf reflectance, transmittance, and fluorescence emission under artificial and natural light conditions [29,30]. We first collected physiological variation using a PAM instrument and upward and downward SIF spectra across 650–800 nm using a FluoWat leaf clip [NO_PRINTED_FORM] under different drought statuses in situ. Furthermore, we investigated the correlations between SIF at different bands and NPQ derived from PAM measurements to study the sensitivity of SIF in response to drought. Finally, a simple approach was proposed to correct the reabsorption effect of chlorophyll on red SIF, which is useful for obtaining a better understanding of red SIF responses to drought.

2. Materials and Methods

2.1. Experimental Protocol and Design

A water stress experiment on maize was conducted in Gucheng, Baoding city, China (39.15°N, 115.74°E), in the summer of 2020. Maize was planted in three 2 m × 4 m split plots on 25 June 2020, and a moveable rain shelter was placed over these plots to protect against rainfall [9]. Three water treatments were imposed on the plots during growth by artificial irrigation, and they are termed the control (C), moderate drought (D1), and severe drought (D2) plots. Plot C was irrigated with 1.7 m^3 in total; D1 was irrigated with 0.7 m^3 in total; and D2 was irrigated with 0.46 m^3 in total before the measurements. To maintain the soil water potential of the C plot, the C plot was again irrigated with 0.4 m^3 on 24 August during the measurements. The soil water potential at a depth of 30 cm was collected using a TEROS-21 sensor (Meter Group, Inc., Pullman, WA, USA) for three plots during data collection. The soil potentials of the three treatments are shown in Table 1. Two field campaigns were conducted in the morning (9:40–11:00) of 21 August and in the afternoon (14:00–15:00) of 25 August.

Table 1. Soil potential (kPa) (Mean ± standard deviation, n = 3) during measurements.

Treatment	Soil Potential (kPa) on 21 August	Soil Potential (kPa) on 25 August
C	−58.07 ± 0.1	−27.47 ± 0.32
D1	−94.81 ± 0.97	−263.47 ± 0.26
D2	−617.06 ± 2.73	−651.28 ± 18.63

2.2. Measurements of Leaf Spectroscopy and PAM Fluorescence In Situ

The scheme of synchronized measurements of leaf spectroscopy and PAM fluorescence is shown in Figure 1. Reflectance (r), transmittance (t), and upward and downward SIF were measured in situ on three leaves attached to their branch on each plot using the FluoWat leaf clip connected to a radiometrically calibrated spectrometer QE pro (Ocean Insight Inc., Dunedin, FL, USA). The QE pro spectrometer covers the spectral range between 350 and 1100 nm with a sampling interval of 0.7 nm and a full width at half maximum of 1.4 nm. The

FluoWat leaf clip has two positions to permit the insertion of the fiber optic, one upward and one downward with respect to the leaf position. The FluoWat leaf clip was mounted on a tripod and was manually positioned so that the incoming solar beam entered the open aperture at a 45° angle relative to the leaf plane. First, a white reference panel was measured to obtain irradiance. Then, upward and downward radiance measurements were collected to calculate r and t. Then, a shortpass filter that cuts off light above 650 nm was inserted into the open aperture to obtain upward reflected radiance (L ↑) and SIF (SIF_λ ↑) and downward transmitted radiance (L ↓) and SIF (SIF_λ ↓) at the same leaf spot. Finally, a white reference panel without a shortpass filter was measured again.

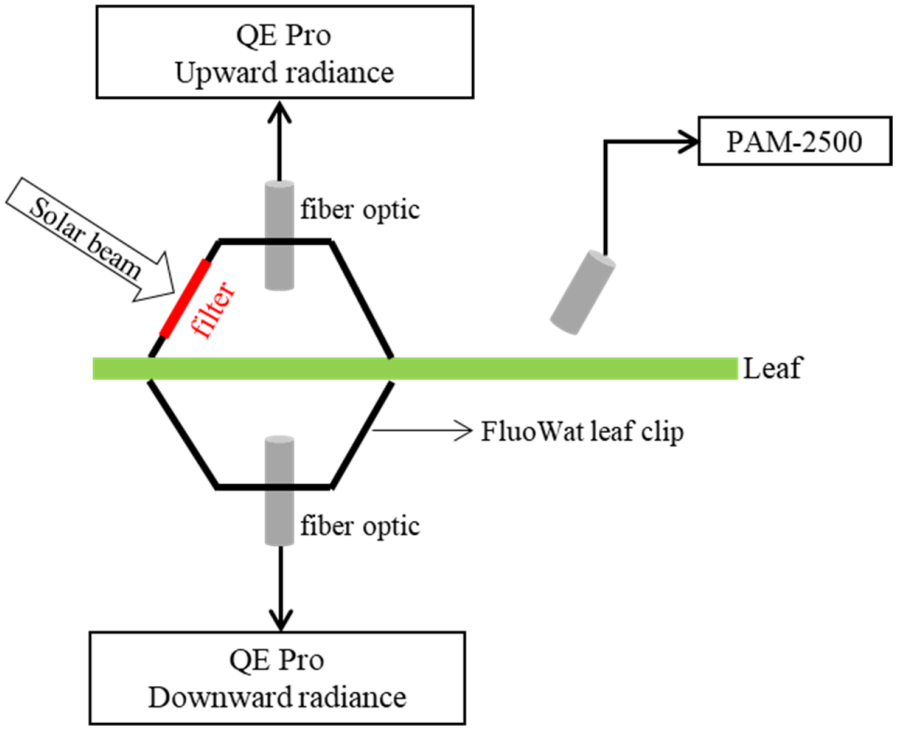

Figure 1. Scheme of measuring spectroscopy and PAM fluorescence on the leaf scale. A FluoWat leaf clip was used to measure reflectance (r), transmittance (t), and sun-induced fluorescence (SIF) in the visible and near-infrared wavelength range (350–1100 nm) by placing a fiber optic either in upward or downward position. After placing the shortpass to restrict incoming PAR to visible wavelengths up to 650 nm, upward and downward SIF are measured. A PAM-2500 fluorometer was used to measure active fluorescence near the clip.

Each leaf was dark-adapted for at least 40 min using a dark acclimation clip (DLC) before PAM measurement. Then, a PAM-2500 (Heinz Walz GmbH, Effeltrich, Bavaria, Germany) fluorometer was used to measure dark-adapted minimal fluorescence (F_o) and maximum fluorescence (F_m), detecting fluorescence radiation above 715 nm using a longpass filter. The values of the maximum PSII quantum yield of photochemistry, $F_v/F_m = (F_m - F_o)/F_m$, were calculated. Subsequently, light-adapted instantaneous steady-state fluorescence (F_t), maximum fluorescence (F'_m) were measured at the sun-exposed position near the DLC on the same leaf. The PSII operating efficiency (ΦP)was estimated using Equation (2) as follows:

$$\Phi P = \frac{F'_m - F_t}{F'_m} \quad (2)$$

Additionally, NPQ was estimated using Equation (3) as follows:

$$NPQ = \frac{F_m - F'_m}{F'_m} \quad (3)$$

2.3. The PAR, APAR, fPAR, and SIF Yield Estimation

To conduct all measurements in a short time, we did not measure the white reference panel with a shortpass filter, so we could not directly obtain the actual incident PAR that excites fluorescence. Therefore, assuming that r and t are the same with or without a filter, we estimated the actual irradiance with $\frac{L\uparrow}{r} * \pi$ and then integrated over 400–650 nm, as shown in Equation (4).

$$PAR = \int_{400}^{650} \frac{L\uparrow}{r} * \pi \, d\lambda \tag{4}$$

Absorbed photosynthetically active radiation ($APAR$) was estimated as follows:

$$APAR = \int_{400}^{650} \frac{L}{r} * \pi * (1 - r - t) d\lambda \tag{5}$$

Then, $fPAR$ at the leaf level can be estimated in Equation (6):

$$fPAR = \frac{APAR}{PAR} \tag{6}$$

In this study, Cab was also measured using a SPAD-502 (Konica-Minolta, Osaka, Japan) on 21 August, and Cab had a good relationship with fPAR (Figure S1). Therefore, we used fPAR to represent Cab variation among different leaves thereafter.

Two approaches for calculating SIF yield (unitless) were used to compare various leaf samples. First, the SIF yield is usually calculated by normalizing the SIF for the APAR if the effect of the escape probability of fluorescence is ignored at the leaf scale [31]. SIF yields are then calculated for the upward, downward and total SIF signals, where the total SIF ($SIF_\lambda tot$) was calculated as the sum of upward and downward SIF. Additionally, Helm et al. found that the SIF yield after normalization by active minimum fluorescence F_o can better reflect the drought response [32]. The minimum fluorescence F_o is also correlated with the Cab and water stress status [33]. Therefore, F_o can reflect the variation in fPAR, and $PAR \times F_o$ can probably be used to represent APAR variation. Therefore, as the second method, the SIF yield was also estimated by normalizing the SIF for $PAR \times F_o$, where the SIF can be $SIF_\lambda \uparrow$, $SIF_\lambda \downarrow$ and $SIF_\lambda tot$.

2.4. Reabsorption Correction of Red SIF

Due to the effect of reabsorption and scattering on the SIF signal, there is a need to convert measured SIF to the photosystem level by using the escape probability ($fesc_\lambda$). At the leaf level, the escape probability of SIF photons from the photosystems to the leaf surface is rather stable in the near infrared region [21]. However, red SIF is much more influenced by the scattering and absorptance effect inside the leaf than near infrared SIF [20]. Therefore, analogous to the p-theory-based escape probability in the NIR region [22], we propose an empirical method to estimate the escape probability from the photosystems to leaf surface at 687 nm ($fesc_{687}$) in Equation (7):

$$fesc_{687} = \frac{r_{687}}{NDVI^2} \tag{7}$$

where NDVI was calculated using the reflectance values at wavelengths 650 nm and 810 nm; r_{687} is the reflectance at 687 nm. In Equation (7), reflectance at 687 nm and NDVI are used to represent the ability of scattering and reabsorption effect, respectively. Although the empirical method has not been validated using radiative transfer model, the obtained $fesc_{687}$ have a good linear relationship with the ratio of downward SIF and upward SIF at 687 nm (see Figure S3 and Section 3.4). Then, the corrected SIF at 687 nm can be calculated in Equation (8):

$$Corrected\ SIF_{687} = \frac{SIF_{687}}{fesc_{687}} \tag{8}$$

where SIF_{687} is the SIF at 687 nm.

2.5. Statistical Analysis

In this study, we used three parameters (NPQ, Φ_P, and F_t/Fo) from PAM measurements to indicate the physiological variations induced by water stress. Due to measurement failure for one leaf sample, there were 17 leaf samples in total during the SIF spectrum analysis. Under stress conditions, NPQ mechanisms are activated, and both ΦP and fluorescence yield decrease proportionally under the action of NPQ [34]. Therefore, we use the NPQ estimated from active fluorescence to represent physiological variation under drought. Then, linear regression model analyses were used to assess the relationships between NPQ and two SIF yields ($\frac{SIF}{APAR}$ and $\frac{SIF}{PAR \times F_o}$) of upward, downward, and total SIF across 660 to 800 nm. The determination coefficients (R^2) were used to assess the ability of the two SIF yields to indicate NPQ. Subsequently, the red (687 nm) and far-red (760 nm) SIF ratios in the downward, upward, and total SIF spectra were also correlated to fPAR and NPQ to study what information these ratios carry. Finally, we assessed how well the adjusted SIF yield ($\frac{SIF}{PAR \times F_o}$) at 687 nm indicated NPQ fluctuation compared with the original SIF yield ($\frac{SIF}{APAR}$) at 760 nm.

3. Results

3.1. Responses of Key Physiological Parameters of PAM to Drought

Four leaf photosynthetic parameters determined from PAM measurements, including F_v/F_m, NPQ, ΦP, and F_t/F_o, under different water conditions, are shown in Figure 2. These values are the mean values of three leaves (except for the D2 measurement on 25 August) in each plot. The values of F_v/F_m decreased slightly under moderate drought (D1) and severe drought (D2) conditions on 21 August and 25 August, respectively. As expected, NPQ was obviously different in response to water treatment and tended to be higher in stressed leaves than in control leaves. Meanwhile, ΦP and F_t/F_o decreased in the treated leaves relative to the control leaves. Here, we used F_t normalized by the dark-adapted basal rate F_o to eliminate the difference between leaves in Cab, leaf structure, etc. [35]. Additionally, the linear relationships between NPQ and ΦP and F_t/F_o of all leaf samples are shown in Figure S2. There were strong negative relationships between NPQ and ΦP and F_t/F_o, with R^2 = 0.89 and R^2 = 0.93, respectively. ΦP had a strong positive correlation with F_t/F_o, with R^2 = 0.86. Therefore, in the subsequent investigation, we employed NPQ as the physiological indicator of the leaf drought response.

3.2. SIF Yield Spectra of the Two Methods and Wavelength-Dependent Correlations with NPQ

To illuminate the different responses of red SIF and far-red SIF to drought, Figure 3 displays the results of total SIF yield spectra of all leaf samples in two methods, $\frac{SIF_\lambda tot}{APAR}$ and $\frac{SIF_\lambda tot}{PAR \times F_o}$ and wavelength-dependent correlations between SIF yield and leaf NPQ. Here, the total SIF ($SIF_\lambda tot$) was calculated as the sum of upward and downward SIF at wavelength λ. Across the range of 660 to 800 nm, two forms of SIF yield spectra typically have two peaks or shoulders in the red at approximately 687 nm and in the far-red at approximately 740 nm, as shown in Figure 3A,B. Specifically, the two forms of SIF yield both presented a better linear relationship with NPQ in the far-red region than in the red region, as shown in Figure 3C,D. Similar to F_t/F_o and ΦP, the SIF yield in the far-red decreased with an increase in NPQ during drought. Interestingly, the linear model between the second SIF yield, $\frac{SIF_\lambda tot}{PAR \times F_o}$, and NPQ had higher determination coefficients (R^2) compared to the determination coefficients between $\frac{SIF_\lambda tot}{APAR}$ and NPQ. In the far-red region, $\frac{SIF_\lambda tot}{PAR \times F_o}$ and NPQ had better and more stable linear relationships with NPQ from 740 nm onward, with R^2 values of approximately 0.7.

Next, the SIF yield spectra estimated in $\frac{SIF}{PAR \times F_o}$ were further investigated for upward ($SIF_\lambda \uparrow$) and downward ($SIF_\lambda \downarrow$) SIF. Figure 4 shows upward and downward SIF yield spectra and their correlations with NPQ. The upward SIF yield exhibits a consistent pattern from 660 to 800 nm, with total SIF yield spectra having two peaks or shoulders in the red and far-red. In contrast to upward SIF, the red peak of the downward SIF yield spectra

almost disappears due to reabsorption of red emitted fluorescence along the optical path through the leaf, which makes the downward SIF yield spectra present a single peak in the far-red region. In the far-red regions, upward and downward SIF yields produce almost the same magnitude, indicating a nearly equal contribution to the total SIF. Similar to the total SIF yield, upward and downward SIF yields also show a better correlation with NPQ in the far-red region and a poor relationship in the red regions. Due to the reduced SIF intensity in red, the downward SIF yield showed a worse linear performance with NPQ in red, with an R^2 close to 0.

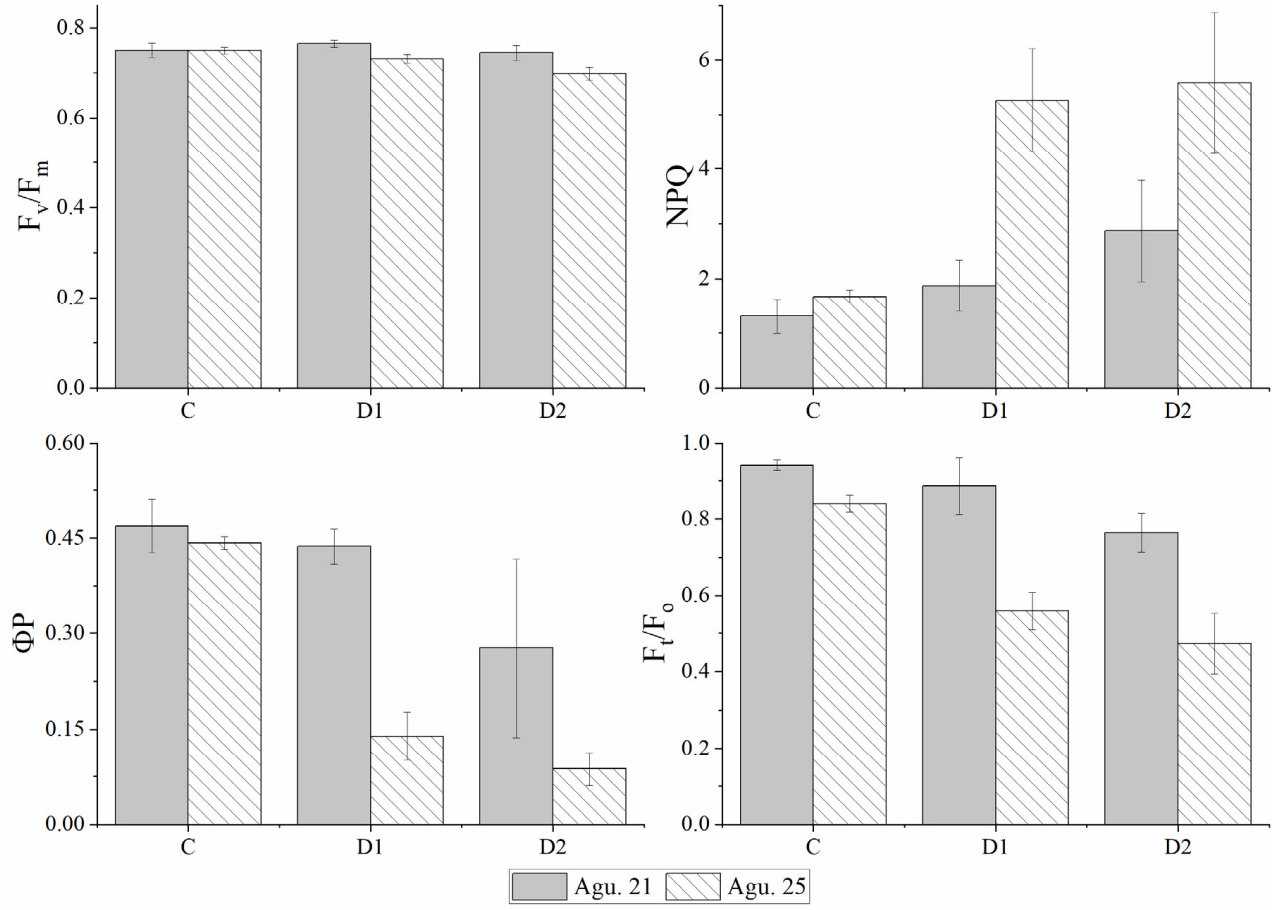

Figure 2. Differences in the key physiological parameters in the three water treatments (mean ± std, n = 3) measured on 21 August and 25 August. Four key parameters are the maximum quantum yield of PSII photochemistry (F_v/F_m), nonphotochemical quenching (NPQ), operating quantum yield of photochemistry in PSII (ΦP), and steady state active fluorescence (F_t) normalized to dark-adapted fluorescence (F_o). C, D1 and D2 indicate the control, moderate drought, and severe drought plots, respectively.

3.3. The Relationship between the Red:Far-Red SIF Ratio and NPQ or fPAR

The above results show that red SIF and far-red SIF yields have different sensitivities in response to drought. Meanwhile, the retrieval of SIF from the background reflected radiation is often conducted using oxygen absorption B and A bands centered at approximately 687–692 nm and 759–770 nm, respectively, when SIF measurements take place outdoors under ambient sunlight. Therefore, we investigated the ratio of red (687 nm) and far-red (760 nm) in the SIF to determine whether the ratio may indicate physiological change or pigment levels to fully extract the information contained in the SIF from limited bands. Figure 5 shows the relationships between the red:far-red ratio and NPQ or fPAR for the downward, upward and total SIF. The downward ratio and NPQ showed a moderate linear performance with R^2 = 0.58, and the upward ratio had a poor linear relationship with NPQ

with R^2 = 0.23. Accordingly, the linear relationship between the red and far-red ratio of total SIF and NPQ had a smaller R^2 than the linear relationship between the red and far-red ratio of total SIF in the downward SIF. The red:far-red ratio of downward SIF was well negatively correlated with fPAR, with R^2 = 0.81. However, the upward ratio shows a low R^2 with fPAR. The ratio of the total SIF had a moderate relationship with fPAR (R^2 = 0.48), which was probably contributed mainly by the downward SIF.

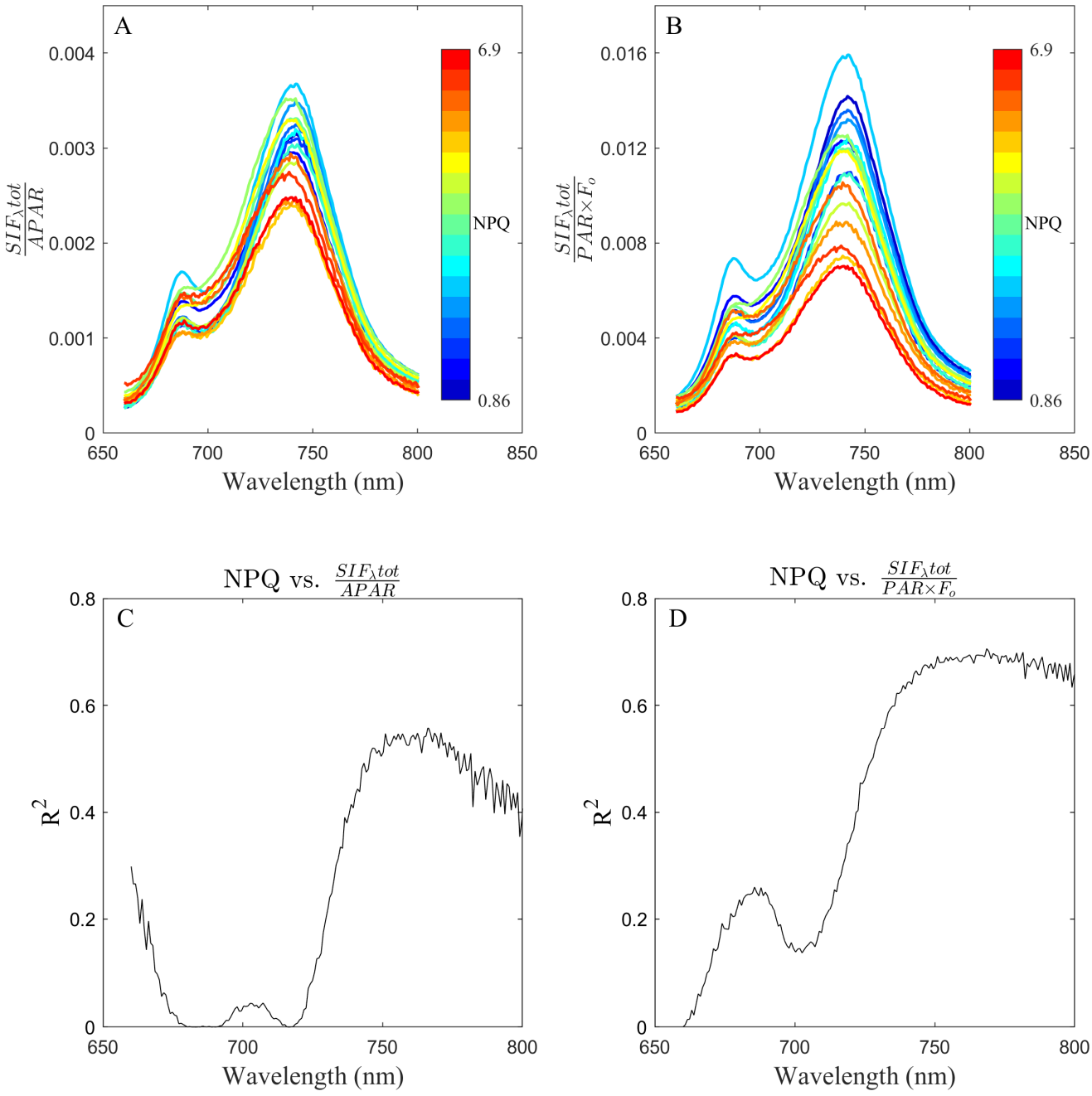

Figure 3. (**A**,**B**) Two forms of total SIF yield $\frac{SIF_\lambda tot}{APAR}$ and $\frac{SIF_\lambda tot}{PAR \times F_o}$ spectra (660~800 nm) for all leaf samples; colored lines represent the nonphotochemical quenching (NPQ) observed in each leaf. (**C**,**D**) Coefficient of determination (R^2) for all wavelengths of SIF yield against NPQ. The coefficient of determination represents the performance of the linear regression.

3.4. Effect of Chl Reabsorption on SIF Spectra

Furthermore, we investigated how drought-induced Cab variation impacts red SIF and far-red SIF responsiveness through reabsorption and scattering effects. The reabsorption

and scattering effects are shown in Figure 6 by calculating the $SIF_\lambda \downarrow / SIF_\lambda \uparrow$ ratio over the whole spectrum as performed by Van Wittenberghe [31]. The red region had low values, which indicate high reabsorption. The minimum of the ratio centered at approximately 683 nm, which is consistent with the red absorption maxima of chlorophyll pigments at these wavelengths [36]. Accordingly, the red peak of the SIF ratio $SIF_{687} \downarrow / SIF_{687} \uparrow$ was strongly correlated with fPAR (R^2 = 0.77). In the far-red region, the ratio had higher values (>0.8) with a relatively stable ratio from 740 nm onward. Far-red region ratios exhibited no correlation with fPAR (R^2 = 0.01). The ratios for the far-red area, however, also vary widely across different leaves, ranging from 0.8 to 1.1.

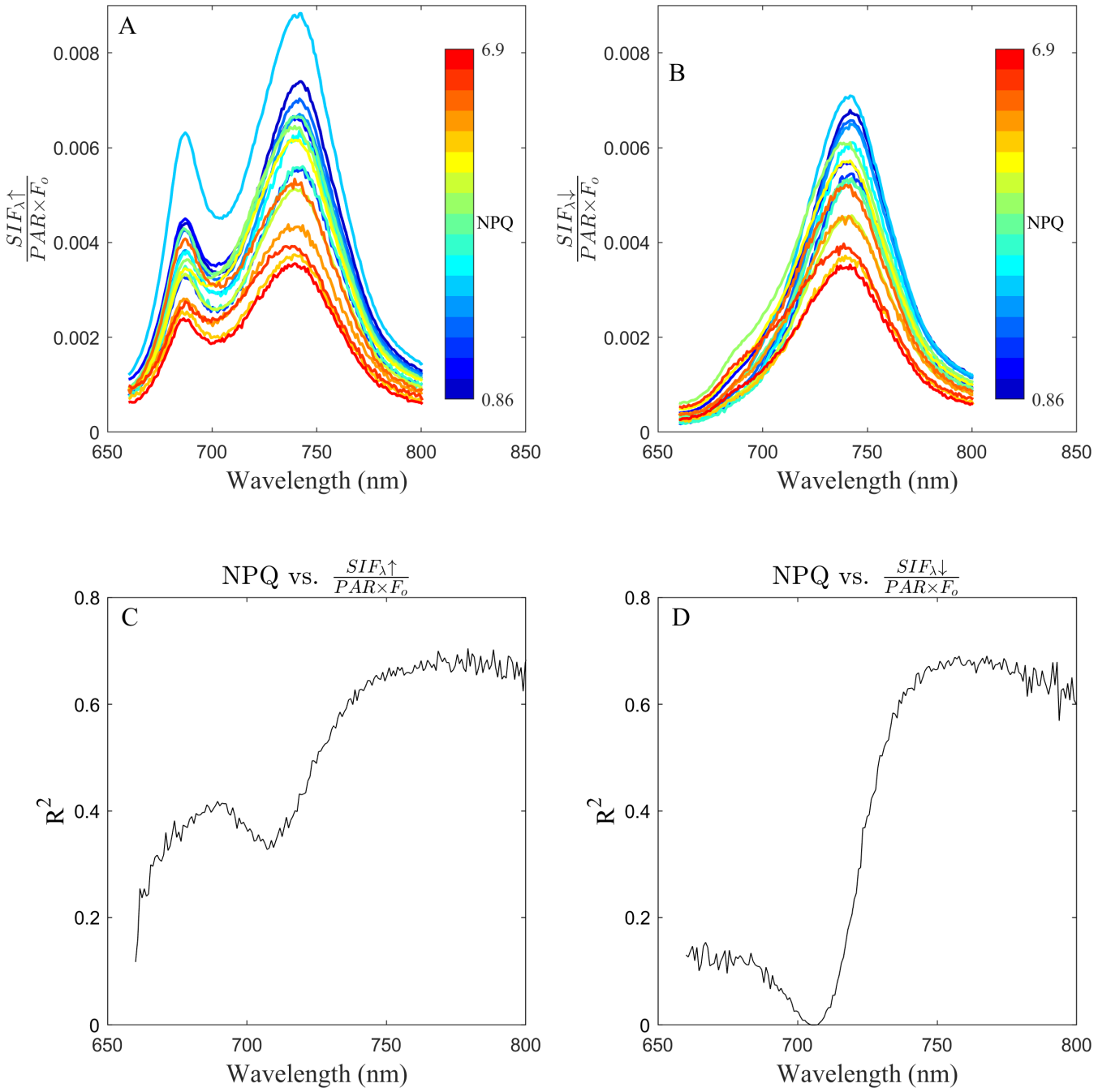

Figure 4. (**A**,**B**) The upward and downward SIF yield ($\frac{SIF_\lambda\uparrow}{PAR\times F_o}$ and $\frac{SIF_\lambda\downarrow}{PAR\times F_o}$) spectra (660~800 nm); colored lines represent the nonphotochemical quenching (NPQ) observed in each leaf. (**C**,**D**) The coefficient of determination (R^2) for all wavelengths of SIF yield against NPQ. The coefficient of determination represents the linear regression performance.

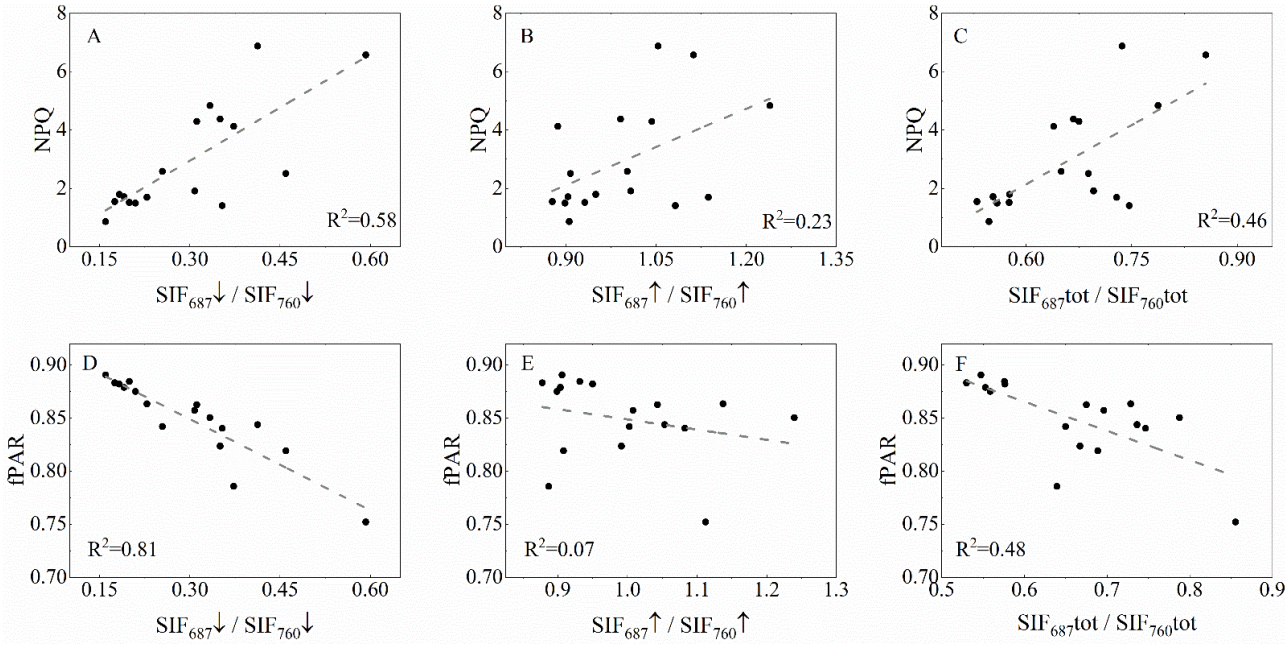

Figure 5. Linear relationships between the red (687 nm): far-red (760 nm) SIF ratio and NPQ for downward (**A**), upward (**B**) and total SIF (**C**). Linear relationships between the red (687 nm): far-red (760 nm) SIF ratio and fPAR for downward (**D**), upward (**E**) and total SIF (**F**). Here, total SIF is calculated as the sum of downward and upward SIF, and fPAR is used to represent the chlorophyll content of leaves.

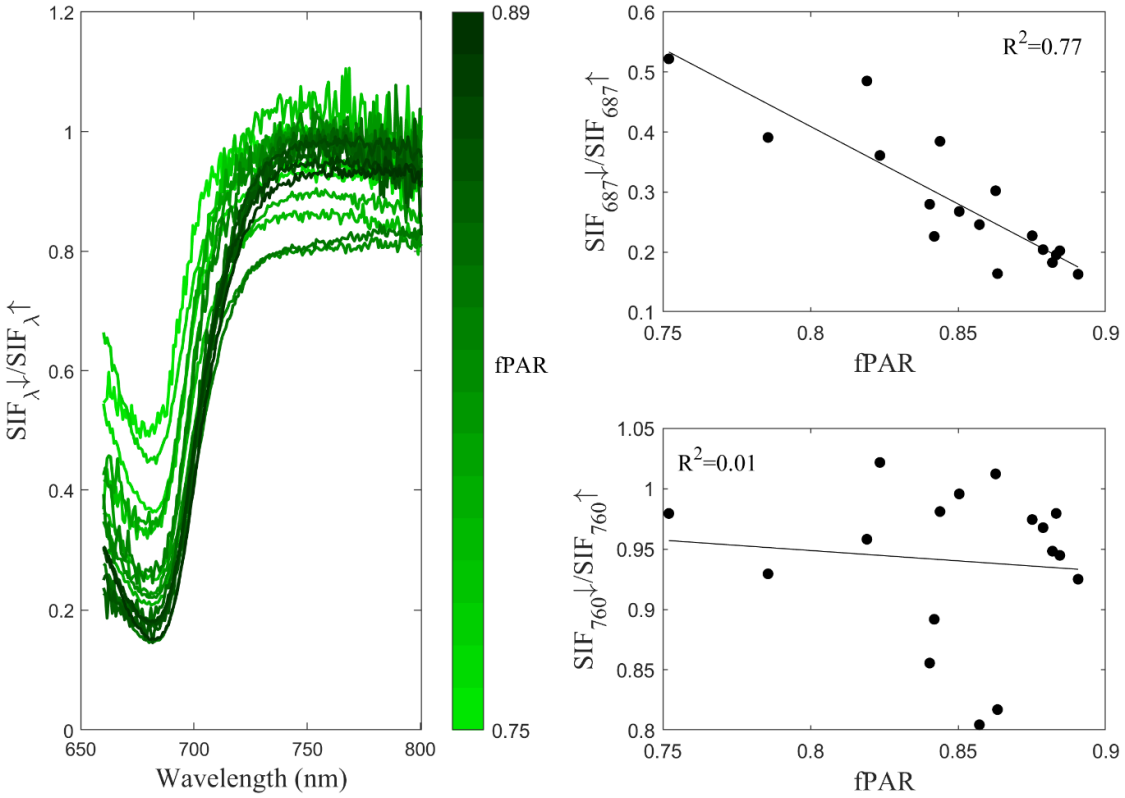

Figure 6. Downward SIF ($SIF_\lambda \downarrow$) and upward SIF ($SIF_\lambda \uparrow$) ratios for the entire SIF spectrum from 660 nm to 800 nm; colored lines represent the fPAR observed in each leaf. Here, fPAR was used to represent chlorophyll a and b content. The right panel shows the linear relationship between the ratio of downward and upward SIF and fPAR at 687 nm and 760 nm, respectively.

3.5. Reabsorption Correction for SIF at 687 nm

Red SIF is much more influenced by the strong chlorophyll absorption effect. To correct this effect, we used an empirical method to estimate the escape probability at 687 nm (Equations (7) and (8)). Then, the performance of the corrected SIF yield at 687 nm with NPQ was compared to the performance of the SIF yield without correction and the SIF yield at 760 nm with NPQ (Figure 7). Red SIF may now more accurately represent NPQ variation, with an increase in the determinate coefficient (R^2) from 0.24 to 0.51 after correction. In contrast to the link between SIF yield at 760 nm and NPQ, the correlation between corrected SIF yield at 687 nm and NPQ is still weaker.

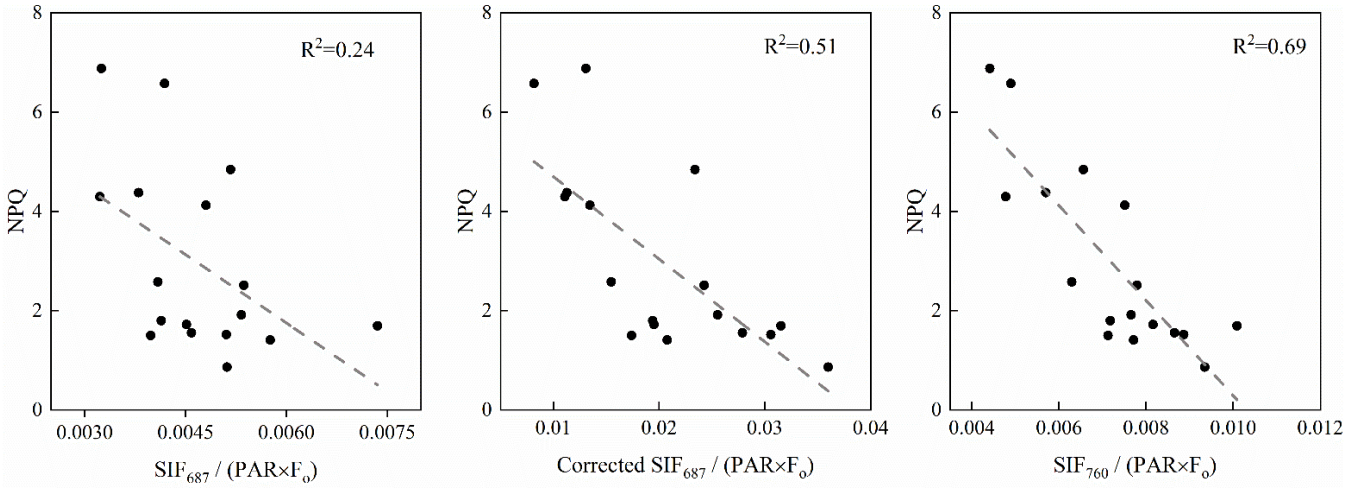

Figure 7. From left to right panel, relationship between the SIF yield at 687 nm before correction, SIF yield at 687 nm after correction and SIF yield at 760 nm and NPQ.

4. Discussion

4.1. Response Sensitivity to Drought of SIF in the Red and Far-Red Regions

Since PSI and PSII determine the SIF signal in the far-red region and PS II predominates in red SIF, red SIF potentially exhibits more responsiveness to changes in physiology [18]. However, the ability of red SIF to track plant physiology is not yet clear. Our aim is to investigate how SIF in red and far-red responses to physiological variation are induced by drought. In this study, our analysis concentrated on the leaf scale to exclude the impact of canopy structure on the SIF signal. We measured the upward and downward SIF spectra across 660 to 800 nm with a FluoWat leaf clip. Then, to retrieve the physiological information included in the SIF signal, the SIF yield was determined without considering the influence of escape probability on SIF intensity. The correlation between SIF yield and NPQ was conducted at different wavelengths. Our findings demonstrate that leaf level SIF in red bands, as opposed to far-red SIF, cannot be well indicate NPQ variation.

Some previous studies have demonstrated that both red and far-red SIF can track seasonal photosynthetic dynamics [18,37]. Nevertheless, their leaf chlorophyll content is also affected in addition to their photosynthetic physiology when plants experience prolonged drought [38]. Drought usually leads to a decrease in Cab in leaves [23]. The partial overlap of the absorption of chlorophyll and the SIF spectrum of a leaf affects the measured fluorescence spectra in the red bands [39]. Therefore, Cab has two effects on SIF emission in the red region: light absorption by influencing fPAR and the proportion of SIF that travels from the photosystems to the leaf surface by affecting escape probability. These two effects of Cab on red SIF emission are opposite. In other words, when Cab falls under drought conditions, light energy absorption falls due to falling fPAR on the one hand, and escape probability rises due to falling reabsorption on the other hand. As opposed to the SIF in the red band, the change in chlorophyll only modifies SIF intensity through fPAR, leaving the escape probability unaffected, as shown in Figure 6. Therefore,

the SIF yields in the red and far-red regions have different sensitivities in response to NPQ under different drought treatments, as shown in Figures 3 and 4, mainly because the physiological information included in the SIF signal cannot be correctly retrieved if the effect of reabsorption on the red SIF is ignored.

The impact of reabsorption on red SIF at the leaf scale must be corrected to properly utilize the physiological information of SIF. By calculating the SIF ratio between downward and upward over the whole fluorescence range, the reabsorption versus scattering effect is better illustrated (Figure 6). Some advances have been made to correct the signal in red based on physical models at the leaf and canopy scales [39,40]. Nevertheless, these models usually require the input reflectance and transmittance of leaves or canopies, which limit their usefulness in remote sensing. Analogous to the p-theory-based escape probability in the NIR region at the canopy scale [22], we proposed a simple reflectance-based approach to estimate the escape probability in red using measurements of the reflectance of the red band and NDVI. The estimated escape probability at 687 nm has a good relationship with the ratio of downward and upward SIF at 687 nm (Figure S3). As shown in Figure 7, the performance of the corrected red SIF in correlating to NPQ has clearly improved. This correction method can help to find more photosynthetic information for remote sensing of SIF in the future. However, due to the small dataset in this study, additional research for various crops and their diverse growth seasons is required to test the generality of conclusions.

4.2. Ability of Red and Far-Red SIF Ratios to Indicate Physiology and Cab Variation under Drought

SIFs in red and far-red bands have different response sensitivities to drought, as discussed above. Additionally, current remote sensing instruments are not capable of retrieving the full SIF spectrum and can only measure emitted photons within narrow atmospheric windows. We expect the ratio to be used as a simple indicator to monitor pigments or physiological changes using remote sensing platforms in the future.

First, the ratio between red and far-red downward SIF may indicate Cab variation because downward SIF in red is fully reabsorbed during fluorescence photos passing through the leaf from the top to the bottom layer, but far-red SIF is not impacted by the effect of reabsorption. Some previous studies demonstrated that the upward fluorescence ratio was well correlated with Cab using laser-induced upward fluorescence [25,27], but our results show that the upward SIF ratio has poor performance in indicating Cab. The difference may result from different leaf inner structures for different species [31]. Although the total SIF ratio shows a moderate relationship with fPAR (R^2 = 0.48), we think the relationship is due mainly to the contribution of the downward SIF to total SIF.

Second, the red and far-red ratio of SIF has limited ability to indicate physiological information (NPQ). The red and far-red ratios of downward and total SIF are moderately correlated with NPQ. The relationship between red:far-red of upward SIF and NPQ is weak. However, we cannot simply assume that red:far-red of downward SIF is mediated by NPQ. The red:far-red ratio of downward SIF has a stronger ability to indicate physiological changes than the ratio of upward SIF. NPQ and Cab probably change proportionally under drought conditions in our experiment. Thus, the increase in NPQ occurs simultaneously with the decrease in Cab. Therefore, the relationship between the SIF ratio and NPQ is still essentially the relationship between the SIF ratio and Cab. To rule out the impact of Cab, the change in the SIF ratio and NPQ must be investigated when there is no noticeable change in Cab under water stress.

4.3. Reasons Why Far-Red SIF Normalized by PAR × F_o Can Better Indicate NPQ

To better interpret the physiological information of SIF signals, we need to decouple the interaction of biochemistry, illumination, and photosynthesis. The SIF yield in the far-red bands was generally calculated by normalizing the SIF using APAR if the escape probability at the leaf scale was not considered [29]. SIF/APAR at 760 nm has been demonstrated to be positively correlated with steady-state fluorescence (F_s) and negatively correlated

with NPQ [32,41]. Furthermore, some studies suggest that both F_s and SIF/APAR were normalized to dark-adapted basal rates (F_o) to consider any difference between leaves due to different leaf structures, Cab, and photodamage, showing a more pronounced drought response [32,35]. However, we find that SIF/PAR/F_o in far-red bands can provide the best indicator for NPQ variation in drought compared with SIF/APAR and SIF/APAR/F_o. One possible reason for this result can be explained by analyzing the information contained in F_o. First, increased dark acclimation F_o was observed under water stress, implying degradation in PSII (D1 protein and other parts of PS) and disruption in energy transfer into the reaction center [42]. Moreover, F_o has been demonstrated to be negatively correlated with Cab [33,43]. Consequently, the F_o includes both photoinhibition and the Cab status of leaves. Therefore, SIF/APAR/F_o would repeatedly eliminate the effect of fPAR, weakening the relationship between the estimated SIF yield and NPQ. Using SIF/PAR/F_o to estimate SIF yield can simultaneously eliminate the effect of fPAR and photoinhibition on SIF signals. However, unless we have solid proof from analyzing other species and more leaf samples, we must temper this interpretation. Another notable issue is that F_o cannot be obtained directly from remote sensing of SIF. An alternative method is to use the SIF signal at low light (early morning) as a proxy for F_o based on geostationary satellites.

5. Conclusions

In this study, we acquired leaf SIF spectral data of upward and downward emissions and photosynthetic parameters from active fluorescence under different drought conditions. The wavelength-dependent link between SIF yield and NPQ was compared. We found that the SIF/PAR/F_o in the far-red region had a strong and stable correlation with NPQ. Drought not only reduces red SIF due to photosynthetic regulation, but it also increases red SIF by lowering chlorophyll content (weakening the reabsorption effect). The co-existence of these two contradictory effects makes the red SIF of leaf scale unable to reliably indicate NPQ. Moreover, the red:far-red ratio in the downward SIF shows a good relationship with Cab, whereas the upward SIF ratio has a poor linear relationship with Cab.

Supplementary Materials: The following supporting information can be downloaded at: https://www.mdpi.com/article/10.3390/rs15041077/s1, Figure S1: Relationship between Cab measured by SPAD-502 and fPAR estimated using leaf absorption; Figure S2: Relationships between nonphotochemical quenching (NPQ) and operating quantum yield of photochemistry in PSII (ΦP), steady-state active fluorescence (F_t) normalized by dark acclimation minimal fluorescence (F_o); Figure S3: Relationships between the ratio of downward SIF and upward SIF at 687 nm and the estimated escape probability at 687 nm.

Author Contributions: Conceptualization, S.X. and Z.L.; methodology, S.X.; formal analysis, Z.L.; investigation, S.X. and Z.L.; resources, S.X., S.H., Z.C., X.H., H.Z. and S.R.; writing—original draft preparation, S.X.; writing—review and editing, Z.L.; visualization, S.X.; supervision, Z.L.; project administration, Z.L.; funding acquisition, Z.L. and S.X. All authors have read and agreed to the published version of the manuscript.

Funding: This research was funded by the Natural Science Foundation of China (grant number 42071402) and the Fundamental Research Funds for the Central Universities (grant number KY-CYXT2022012) during this work.

Acknowledgments: We thank the anonymous reviewers for their constructive comments. We are also grateful to the Natural Science Foundation of China and Fundamental Research Funds for the Central Universities for their support.

Conflicts of Interest: The authors declare no conflict of interest.

References

1. Leng, G.; Tang, Q.; Rayburg, S. Climate Change Impacts on Meteorological, Agricultural and Hydrological Droughts in China. *Glob. Planet Chang.* **2015**, *126*, 23–34. [CrossRef]
2. Cook, B.I.; Mankin, J.S.; Anchukaitis, K.J. Climate Change and Drought: From Past to Future. *Curr. Clim. Chang. Rep.* **2018**, *4*, 164–179. [CrossRef]

3. Barnabás, B.; Jäger, K.; Fehér, A. The Effect of Drought and Heat Stress on Reproductive Processes in Cereals. *Plant Cell Environ.* **2008**, *31*, 11–38. [CrossRef] [PubMed]
4. Alley, W.M. The Palmer Drought Severity Index: Limitations and Assumptions. *J. Appl. Meteorol. Climatol.* **1984**, *23*, 1100–1109. [CrossRef]
5. Wardlow, B.D.; Tadesse, T.; Brown, J.F.; Callahan, K.; Swain, S.; Hunt, E. Vegetation Drought Response Index an Integration of Satellite, Climate, and Biophysical Data. In *Remote Sensing of Drought: Innovative Monitoring Approaches*; Wardlow, B.D., Anderson, M.C., Verdin, J.P., Eds.; CPC Press: Boca Raton, FL, USA, 2012; pp. 51–74.
6. Govindjee, G. Chlorophyll a Fluorescence: A Bit of Basics and History. In *Chlorophyll a Fluorescence: A Signature of Photosynthesis*; Springer: Dordrecht, Switzerland, 2004; pp. 1–42.
7. Song, L.; Guanter, L.; Guan, K.; You, L.; Huete, A.; Ju, W.; Zhang, Y. Satellite Sun-induced Chlorophyll Fluorescence Detects Early Response of Winter Wheat to Heat Stress in the Indian Indo-Gangetic Plains. *Glob. Chang. Biol.* **2018**, *24*, 4023–4037. [CrossRef]
8. Ni, Z.; Liu, Z.; Huo, H.; Li, Z.-L.; Nerry, F.; Wang, Q.; Li, X. Early Water Stress Detection Using Leaf-Level Measurements of Chlorophyll Fluorescence and Temperature Data. *Remote Sens.* **2015**, *7*, 3232–3249. [CrossRef]
9. Xu, S.; Liu, Z.; Zhao, L.; Zhao, H.; Ren, S. Diurnal Response of Sun-Induced Fluorescence and PRI to Water Stress in Maize Using a Near-Surface Remote Sensing Platform. *Remote Sens.* **2018**, *10*, 1510. [CrossRef]
10. Liu, L.; Yang, X.; Zhou, H.; Liu, S.; Zhou, L.; Li, X.; Yang, J.; Han, X.; Wu, J. Evaluating the Utility of Solar-Induced Chlorophyll Fluorescence for Drought Monitoring by Comparison with NDVI Derived from Wheat Canopy. *Sci. Total Environ.* **2018**, *625*, 1208. [CrossRef]
11. Cao, J.; An, Q.; Zhang, X.; Xu, S.; Si, T.; Niyogi, D. Is Satellite Sun-Induced Chlorophyll Fluorescence More Indicative than Vegetation Indices under Drought Condition? *Sci. Total Environ.* **2021**, *792*, 148396. [CrossRef] [PubMed]
12. Zarco-Tejada, P.J.; González-Dugo, V.; Berni, J.A.J. Fluorescence, Temperature and Narrow-Band Indices Acquired from a UAV Platform for Water Stress Detection Using a Micro-Hyperspectral Imager and a Thermal Camera. *Remote Sens. Environ.* **2012**, *117*, 322–337. [CrossRef]
13. Sun, Y.; Fu, R.; Dickinson, R.; Joiner, J.; Frankenberg, C.; Gu, L.; Xia, Y.; Fernando, N. Drought Onset Mechanisms Revealed by Satellite Solar-induced Chlorophyll Fluorescence: Insights from Two Contrasting Extreme Events. *J. Geophys. Res. Biogeosci.* **2015**, *120*, 2427–2440. [CrossRef]
14. Genty, B.; Wonders, J.; Baker, N.R. Non-Photochemical Quenching of Fo in Leaves Is Emission Wavelength Dependent: Consequences for Quenching Analysis and Its Interpretation. *Photosynth. Res.* **1990**, *26*, 133–139. [CrossRef] [PubMed]
15. Franck, F.; Juneau, P.; Popovic, R. Resolution of the Photosystem I and Photosystem II Contributions to Chlorophyll Fluorescence of Intact Leaves at Room Temperature. *Biochimica et Biophysica Acta (BBA)-Bioenergetics* **2002**, *1556*, 239–246. [CrossRef]
16. Hasegawa, M.; Shiina, T.; Terazima, M.; Kumazaki, S. Selective Excitation of Photosystems in Chloroplasts Inside Plant Leaves Observed by Near-Infrared Laser-Based Fluorescence Spectral Microscopy. *Plant Cell Physiol.* **2010**, *51*, 225–238. [CrossRef]
17. Magney, T.S.; Frankenberg, C.; Köhler, P.; North, G.; Davis, T.S.; Dold, C.; Dutta, D.; Fisher, J.B.; Grossmann, K.; Harrington, A. Disentangling Changes in the Spectral Shape of Chlorophyll Fluorescence: Implications for Remote Sensing of Photosynthesis. *J. Geophys. Res. Biogeosci.* **2019**, *124*, 1491–1507. [CrossRef]
18. Duan, W.; Liu, X.; Chen, J.; Du, S.; Liu, L.; Jing, X. Investigating the Performance of Red and Far-Red SIF for Monitoring GPP of Alpine Meadow Ecosystems. *Remote Sens.* **2022**, *14*, 2740. [CrossRef]
19. Guanter, L.; Zhang, Y.; Jung, M.; Joiner, J.; Voigt, M.; Berry, J.A.; Frankenberg, C.; Huete, A.R.; Zarco-Tejada, P.; Lee, J.-E.; et al. Global and Time-Resolved Monitoring of Crop Photosynthesis with Chlorophyll Fluorescence. *Proc. Natl. Acad. Sci. USA* **2014**, *111*, E1327–E1333. [CrossRef]
20. Liu, X.; Liu, L.; Hu, J.; Guo, J.; Du, S. Improving the Potential of Red SIF for Estimating GPP by Downscaling from the Canopy Level to the Photosystem Level. *Agric. For. Meteorol.* **2020**, *281*, 107846. [CrossRef]
21. Liu, Z.; Zhao, F.; Liu, X.; Yu, Q.; Wang, Y.; Peng, X. Remote Sensing of Environment Direct Estimation of Photosynthetic CO_2 Assimilation from Solar-Induced Chlorophyll Fluorescence (SIF). *Remote Sens. Environ.* **2022**, *271*, 112893. [CrossRef]
22. Yang, P.; Van Der Tol, C. Linking Canopy Scattering of Far-Red Sun-Induced Chlorophyll Fluorescence with Reflectance. *Remote Sens. Environ.* **2018**, *209*, 456–467. [CrossRef]
23. Mayoral, M.L.; Atsmon, D.; Shimshi, D.; Gromet-Elhanan, Z. Effect of Water Stress on Enzyme Activities in Wheat and Related Wild Species: Carboxylase Activity, Electron Transport and Photophosphorylation in Isolated Chloroplasts. *Funct. Plant Biol.* **1981**, *8*, 385–393. [CrossRef]
24. Kuroda, M.; Oaiawa, T.; Imagawa, H. Changes in Chloroplast Peroxidase Activities in Relation to Chlorophyll Loss in Barley Leaf Segments. *Physiol. Plant* **1990**, *80*, 555–560. [CrossRef]
25. Lichtenthaler, H.K.; Wenzel, O.; Buschmann, C.; Gitelson, A. Plant Stress Detection by Reflectance and Fluorescence. *Ann. N. Y. Acad. Sci.* **1998**, *851*, 271–285. [CrossRef]
26. Ač, A.; Malenovský, Z.; Olejníčková, J.; Gallé, A.; Rascher, U.; Mohammed, G. Meta-Analysis Assessing Potential of Steady-State Chlorophyll Fluorescence for Remote Sensing Detection of Plant Water, Temperature and Nitrogen Stress. *Remote Sens. Environ.* **2015**, *168*, 420–436. [CrossRef]
27. Gitelson, A.A.; Buschmann, C.; Lichtenthaler, H.K. Leaf Chlorophyll Fluorescence Corrected for Re-Absorption by Means of Absorption and Reflectance Measurements. *J. Plant Physiol.* **1998**, *152*, 283–296. [CrossRef]

28. Buschmann, C. Variability and Application of the Chlorophyll Fluorescence Emission Ratio Red/Far-Red of Leaves. *Photosynth. Res.* **2007**, *92*, 261–271. [CrossRef]
29. van Wittenberghe, S.; Alonso, L.; Verrelst, J.; Hermans, I.; Delegido, J.; Veroustraete, F.; Valcke, R.; Moreno, J.; Samson, R. Upward and Downward Solar-Induced Chlorophyll Fluorescence Yield Indices of Four Tree Species as Indicators of Traffic Pollution in Valencia. *Environ. Pollut.* **2013**, *173*, 29–37. [CrossRef]
30. Alonso, L.; Gomezchova, L.; Vilafrances, J.; Amoroslopez, J.; Guanter, L.; Calpe, J.; Moreno, J. Sensitivity Analysis of the Fraunhofer Line Discrimination Method for the Measurement of Chlorophyll Fluorescence Using a Field Spectroradiometer. In Proceedings of the International Geoscience and Remote Sensing Symposium, Barcelona, Spain, 23–28 July 2007; pp. 3756–3759.
31. Van Wittenberghe, S.; Alonso, L.; Verrelst, J.; Moreno, J.; Samson, R. Bidirectional Sun-Induced Chlorophyll Fluorescence Emission Is Influenced by Leaf Structure and Light Scattering Properties—A Bottom-up Approach. *Remote Sens. Environ.* **2015**, *158*, 169–179. [CrossRef]
32. Helm, L.T.; Shi, H.; Lerdau, M.T.; Yang, X. Solar-Induced Chlorophyll Fluorescence and Short-Term Photosynthetic Response to Drought. *Ecol. Appl.* **2020**, *30*, e02101. [CrossRef]
33. Hazrati, S.; Tahmasebi-Sarvestani, Z.; Modarres-Sanavy, S.A.M.; Mokhtassi-Bidgoli, A.; Nicola, S. Effects of Water Stress and Light Intensity on Chlorophyll Fluorescence Parameters and Pigments of *Aloe vera* L. *Plant Physiol. Biochem.* **2016**, *106*, 141–148. [CrossRef]
34. Porcar-Castell, A.; Tyystjärvi, E.; Atherton, J.; van der Tol, C.; Flexas, J.; Pfündel, E.E.; Moreno, J.; Frankenberg, C.; Berry, J.A. Linking Chlorophyll a Fluorescence to Photosynthesis for Remote Sensing Applications: Mechanisms and Challenges. *J. Exp. Bot.* **2014**, *65*, 4065–4095. [CrossRef]
35. Flexas, J.; Escalona, J.M.; Evain, S.; Gulías, J.; Moya, I.; Osmond, C.B.; Medrano, H. Steady-state Chlorophyll Fluorescence (Fs) Measurements as a Tool to Follow Variations of Net CO2 Assimilation and Stomatal Conductance during Water-stress in C3 Plants. *Physiol. Plant* **2002**, *114*, 231–240. [CrossRef]
36. Karcz, D.; Boroń, B.; Matwijczuk, A.; Furso, J.; Staroń, J.; Ratuszna, A.; Fiedor, L. Lessons from Chlorophylls: Modifications of Porphyrinoids Towards Optimized Solar Energy Conversion. *Molecules* **2014**, *19*, 15938–15954. [CrossRef]
37. Zhang, C.; Atherton, J.; Peñuelas, J.; Filella, I.; Kolari, P.; Aalto, J.; Ruhanen, H.; Bäck, J.; Porcar-Castell, A. Do All Chlorophyll Fluorescence Emission Wavelengths Capture the Spring Recovery of Photosynthesis in Boreal Evergreen Foliage? *Plant Cell Environ.* **2019**, *42*, 3264–3279. [CrossRef]
38. Li, Y.; Song, H.; Zhou, L.; Xu, Z.; Zhou, G. Vertical Distributions of Chlorophyll and Nitrogen and Their Associations with Photosynthesis under Drought and Rewatering Regimes in a Maize Field. *Agric. For. Meteorol.* **2019**, *272–273*, 40–54. [CrossRef]
39. Agati, G.; Fusi, F.; Mazzinghi, P.; di Paola, M.L. A Simple Approach to the Evaluation of the Reabsorption of Chlorophyll Fluorescence Spectra in Intact Leaves. *J. Photochem. Photobiol. B* **1993**, *17*, 163–171. [CrossRef]
40. Romero, J.M.; Cordon, G.B.; Lagorio, M.G. Modeling Re-Absorption of Fluorescence from the Leaf to the Canopy Level. *Remote Sens. Environ.* **2018**, *204*, 138–146. [CrossRef]
41. Magney, T.S.; Frankenberg, C.; Fisher, J.B.; Sun, Y.; North, G.B.; Davis, T.S.; Kornfeld, A.; Siebke, K. Connecting Active to Passive Fluorescence with Photosynthesis: A Method for Evaluating Remote Sensing Measurements of Chl Fluorescence. *New Phytol.* **2017**, *215*, 1594–1608. [CrossRef]
42. Calatayud, A.; Roca, D.; Martínez, P.F. Spatial-Temporal Variations in Rose Leaves under Water Stress Conditions Studied by Chlorophyll Fluorescence Imaging. *Plant Physiol. Biochem.* **2006**, *44*, 564–573. [CrossRef]
43. Fu, W.; Li, P.; Wu, Y. Effects of Different Light Intensities on Chlorophyll Fluorescence Characteristics and Yield in Lettuce. *Sci. Hortic.* **2012**, *135*, 45–51. [CrossRef]